

Appendices

APPENDIX A

Data Selection

A.0.1 Differential Yield Determination

```
1 # Add files to TChain and check if all 8 files were found
2 def add_files_to_chain(chain, directory, tree_name):
3     energy = next((e for e in ENERGIES if e in directory), "Unknown
4     Energy")
5     pdf = next((p for p in PDFs if p in directory), "Unknown PDF")
6
7     if chain.Add(f"{directory}/SimulationResults3_thread*.root") == 8:
8         print(f"All {NUM_THREADS} files for {energy} - {pdf} were found.
9         ")
10    else:
11        print(f"Error: Expected to find 8 files for {energy} - {pdf}!")
12
13 # Draw and save histograms
14 def draw_and_save_histogram(chain, histogram, directory, event_count,
15    today):
16     pTyield = rt.TCanvas("pTyield", "pT", 100, 15, 900, 500)
17     pTyield.SetLogy()
18
19     # Determine the appropriate draw command based on the histogram name
20     # e.g., histogram name: DNDPT_PYTHIA8_5TEV_NNPDF30_PIONS
21
22     if "_TOTAL_NOCUTS" in histogram.GetName():
```

```

21 chain.Draw(f"pT >> {histogram.GetName()}")
22 elif "_TOTAL" in histogram.GetName():
23     chain.Draw(f"pT >> {histogram.GetName()}", "eta > -4.0 && eta <
24     -2.5 && p > 4")
25 else:
26     flavour = PARTICLE_FLAVOUR_MAP.get(histogram.GetName().split("_")
27     )[-1], None)
28     if flavour:
29         chain.Draw(f"pT >> {histogram.GetName()}", f"eta > -4.0 &&
30         eta < -2.5 && flavour == {flavour} && p > 4")

    histogram.SaveAs(f"{directory}/{histogram.GetName()}_{event_count}_{
today}.root")
    return histogram

```

Listing A.1 Muon source histogram code snippet

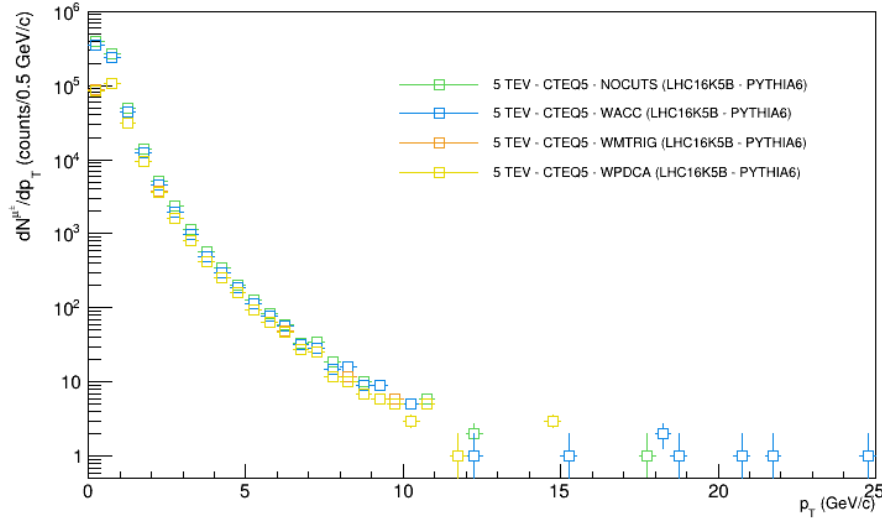


Fig. A.1 This plot illustrates the differential yield of all muons as a function of transverse momentum, generated using the PYTHIA 8 event generator with the CTEQ5 PDF, within the AliRoot framework for the ALICE experiment at a $\sqrt{s} = 5$ TeV.

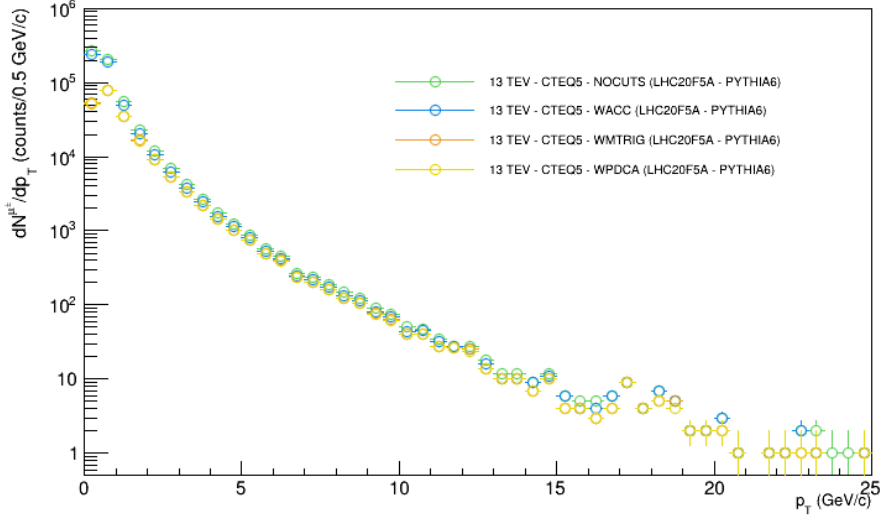


Fig. A.2 This plot displays the differential yield of all muons as a function of transverse momentum, produced by the PYTHIA 6 event generator using the CTEQ5 parton distribution function within the AliRoot framework from the ALICE experiment at a center-of-mass energy of 13 TeV.

A.0.1.1 The Event Analysis Loop

The `UserExec()` is called for every event in the AOD file.

```
1 void AliAnalysisTaskMyMuonAncestor::UserExec(Option_t *){
2     // analysis loop goes here
3     PostData(1, fOutputList); // runs after analysis loop is complete
4 }
```

Listing A.2 Event generation loop

`UserExec()` is the core of the analysis task and is where the muon selection and analysis are done. After the analysis loop is complete, `PostData(1, fOutputList)` posts the contents of `fOutputList` to ensure that the output is written to the output file.

A.0.1.1.1 Event Headers and Trigger Information One critical piece of meta-data retrieved from the AOD is the header information, which contains various high-level details about the event, such as the run number, event number, and trigger information. Trigger data is important because triggers for part of the acceptance criteria for muons when analysing MC data with accurate detector response.

```
1 AliAODHeader *aodheader=dynamic_cast<AliAODHeader*>(fAOD->GetHeader());
2 fMCHHeader = (AliAODMCHHeader*)fAOD->FindListObject(AliAODMCHHeader::
    StdBranchName());
```

```

3 fMCArray = dynamic_cast<TClonesArray*>(fAOD->FindListObject(
    AliAODMCParticle::StdBranchName()));
4 TString firedtrigger = aodheader->GetFiredTriggerClasses();
5
6 // Simplify trigger selection
7 std::vector<std::pair<std::string, bool>> triggers = {{"MB1", false}, {"
    MULU", false}, {"MULL", false}, {"MULow", false}, {"MUHigh", false}};
8
9 for(auto &trigger : triggers) {
10     trigger.second = firedtrigger.Contains(trigger.first.c_str());
11     if (trigger.second) fNTrig->Fill((&trigger - &triggers[0])+1.);
12 }
13
14 // Always fill for index 0
15 fNTrig->Fill(0);
16
17 // Handle MC Event
18 fMCEvent = MCEvent();
19 if(!fMCEvent){
20     AliError(" MC Event not found");
21     return;
22 }
23
24 // Get the number of tracks
25 Int_t nTracksMC = fAOD->GetNumberOfTracks();

```

Listing A.3 Trigger and MC event data handling

1. `AliAODHeader *aodheader =`
`dynamic_cast<AliAODHeader*>(fAOD->GetHeader()):` This statement retrieves the header of the current event from the AOD file. This header, which is stored as an `AliAODHeader` object in the `aodheader` variable, encapsulates the event's metadata, including its run number, event number, and timestamp.
2. `fMCHeader =`
`(AliAODMCHHeader*)fAOD->FindListObject(AliAODMCHHeader::StdBranchName()):`
This line retrieves the MC header. It calls the `FindListObject()` function with `AliAODMCHHeader::StdBranchName()` as an argument, indicating the branch containing the MC header. The MC header, stored in `fMCHeader`, holds information about the settings of the MC event generator used to simulate the events in the AOD.
3. `fMCArray`
`= dynamic_cast<TClonesArray*>(fAOD->FindListObject(...)):` This line also uses the `FindListObject()` function, but this time to retrieve the array of MC

particles. Stored in `fMCArray` as a `TClonesArray` object, these particles provide various parameters such as momentum, energy, and charge.

4. `TString firedtrigger = aodheader->GetFiredTriggerClasses()`: Here, the function `GetFiredTriggerClasses()` is called on the `aodheader` object to get a list of the triggers that were fired in the current event. This list, stored as a `TString` object in `firedtrigger`, helps to identify the conditions under which the event was captured.
5. The vector `std::vector<std::pair<std::string, bool>>triggers` holds the string identifier and the boolean flag for each relevant trigger. The loop `for(auto &trigger : triggers)` is used to iterate over each trigger pair in the vector, checking whether the fired triggers from the event contain the string identifier of the current pair. If they do, the corresponding boolean flag is set to `true`.
6. `fMCEvent = MCEvent()` and `if(!fMCEvent){...}`: This segment fetches the MC event, storing it in `fMCEvent`. If the MC event is not found, it logs an error message and returns, halting further processing in the current iteration.
7. `Int_t nTracksMC = fAOD->GetNumberOfTracks()`: This line retrieves the number of tracks in the event from the AOD file. This is crucial information, as these tracks represent the particles produced in the event.

A.1 Event Selection

```
1  \\ select the muons of interest
2  Bool_t IsWithinMuonSpectrometerAcceptance(AliAODTrack* track) {
3      if(track->Eta() < -4 || track->Eta() > -2.5) return kFALSE;
4      Double_t Theta = track->Theta() * TMath::RadToDeg();
5      if(Theta < 171 || Theta > 178) return kFALSE;
6      if(track->GetRAtAbsorberEnd() < 17.6 || track->GetRAtAbsorberEnd() >
7          89.5) return kFALSE;
8      return kTRUE;
9  }
10
11 Bool_t IsMuonTrackMatchingTrigger(AliAODTrack* track) {
12     return (track->GetMatchTrigger() >= 1); // At least matches, even if
13     it does not pass the pt cut
14 }
15
16 Bool_t IsPDCASelected(AliAODTrack* track) {
17     return fMuonTrackCuts->IsSelected(track); // pDCA cuts applied here
18 }
```

```

18
19 void CalculatePDCA(AliAODTrack* track) {
20     Double_t pTotMean = fMuonTrackCuts->GetAverageMomentum(track);
21     TVector3 dcaAtVz = fMuonTrackCuts->GetCorrectedDCA(track);
22     Double_t pDCA = pTotMean * dcaAtVz.Mag();
23     // Further processing of pDCA if needed
24 }

```

Listing A.4 Analysis Loop Initialization

A.1.0.0.1 Differential Yield Using the `AliUtilityMuonAncestor` methods, we determine the muon ancestors and fill their respective histograms:

```

1
2 // Updated the function pointer array to include the new functions.
3 Bool_t (*isMuonTypeFuncs[kNumMuonTypes])(AliAODTrack*, AliAODEvent*) = {
4     &AliAODTrack::IsMuon, &AliAODTrack::IsBeautyMu, &AliAODTrack::
5     IsBeautyChainMu, &AliAODTrack::IsBJpsiMu,
6     &AliAODTrack::IsCharmMu, &AliAODTrack::IsCharmChainMu, &AliAODTrack
7     ::IsDecayMu, &AliAODTrack::IsHadron,
8     &AliAODTrack::IsQuarkoniumMu, &AliAODTrack::IsSecondaryMu, &
9     AliAODTrack::IsUnidentified,
10    &AliAODTrack::IsWBosonMu, &AliAODTrack::IsZBosonMu, &IsPionMu, &
11    IsKaonMu
12 };
13
14 // Updated histogram names array to include new histograms for the new
15 // functions.
16 const char* muonHistNames[kNumMuonTypes] = {
17     "fHistSource_IsMuon", "fHistSource_IsBeautyMu", "
18     fHistSource_IsBeautyChainMu", "fHistSource_IsBJpsiMu",
19     "fHistSource_IsCharmMu", "fHistSource_IsCharmChainMu", "
20     fHistSource_IsDecayMu", "fHistSource_IsHadron",
21     "fHistSource_IsQuarkoniumMu", "fHistSource_IsSecondaryMu", "
22     fHistSource_IsUnidentified",
23     "fHistSource_IsWBosonMu", "fHistSource_IsZBosonMu", "
24     fHistSource_IsPionMu", "fHistSource_IsKaonMu"
25 };
26
27 for (int i = 0; i < kNumMuonTypes; ++i) {
28     if ((fTrack->*isMuonTypeFuncs[i])(fTrack, fMCEvent)) {
29         fMuSources->Fill(i);
30         double pt = fTrack->Pt();
31         ((THnSparseF*)fOutputList->FindObject(muonHistNames[i]))->Fill(&
32         pt);
33         if (i == 6 && !fTrack->IsBeautyChainMu(fTrack, fMCEvent) && !
34         fTrack->IsCharmChainMu(fTrack, fMCEvent)) {

```

```
24         fDecayMuPtWpDCA->Fill(pt);  
25     }  
26 }  
27 }
```

Listing A.5 Analysis Loop Initialization

1. Constant Definitions: This line defines an integer constant `kNumMuonTypes` with a value of 15. This constant represents the total number of muon type functions used.
2. Function Pointer Array: This line defines an array of function pointers named `isMuonTypeFuncs`. Each element of the array points to a function that takes in two arguments (`AliAODTrack*` and `AliAODEvent*`) and returns a boolean. The array contains 15 pointers corresponding to different functions that check various properties or origins of muons.
3. Histogram Names Array: This line defines an array of string literals named `muonHistNames`. Each string represents the name of a histogram associated with the corresponding muon type function.
4. Loop Over Muon Types and Fill Histograms: The loop iterates over each of the muon type functions in `isMuonTypeFuncs`. For each iteration:
 - (a) It checks if the muon (represented by `fTrack`) matches the criteria specified by the current muon type function. This is done by calling the function using the syntax `(fTrack->isMuonTypeFuncs[i])(fTrack, fMCEvent)`.
 - (b) If the criteria are met (if the condition is true):
 - i. It fills the `fMuSources` histogram with the index `i` (corresponding to the current muon type).
 - ii. It then gets the transverse momentum of the muon with `fTrack->Pt()` and stores it in `pt`.
 - iii. Using the current histogram name from `muonHistNames`, it finds the corresponding histogram in `fOutputList` and fills it with the muon's transverse momentum.
 - iv. There is a special case: if the current muon type index is 6 (`i == 6`) and the muon does not match the criteria for `IsBeautyChainMu` and `IsCharmChainMu`, it fills the `fDecayMuPtWpDCA` histogram with the muon's transverse momentum.

In this work, we have also created two new methods `IsPionMu()` and `IsKaonMu()`, which

are not implemented in the `AliUtilityMuonAncestor` class, to match the implementation of the standalone PYTHIA analysis and have separate histograms for muons from decays of primary pions and kaons.

```

1   if (mcParticle && TMath::Abs(mcParticle->PdgCode()) == 13) {
2       Int_t imother = mcParticle->GetMother();
3       while (imother >= 0) {
4           const AliVParticle* part = fMCEvent->GetTrack(imother);
5           Int_t absPdg = TMath::Abs(part->PdgCode());
6           Bool_t isPrimary = AliAnalysisMuonUtility::IsPrimary(part,
fmCEvent);
7           if (isPrimary && absPdg == 211) {
8               return kTRUE;
9           }
10          imother = part->GetMother();
11      }
12  }
13  return kFALSE;
14 }
15
16 Bool_t IsKaonMu(AliAODTrack* mcParticle, AliAODEvent* fMCEvent) {
17     if (mcParticle && TMath::Abs(mcParticle->PdgCode()) == 13) {
18         Int_t imother = mcParticle->GetMother();
19         while (imother >= 0) {
20             const AliVParticle* part = fMCEvent->GetTrack(imother);
21             Int_t absPdg = TMath::Abs(part->PdgCode());
22             Bool_t isPrimary = AliAnalysisMuonUtility::IsPrimary(part,
fmCEvent);
23             if (isPrimary && absPdg == 321) {
24                 return kTRUE;
25             }
26             imother = part->GetMother();
27         }
28     }
29     return kFALSE;
30 }

```

Listing A.6 Analysis Loop Initialization

The functions work by checking if `mcParticle` is not null and its PDG code is 13 (muon). The loop traces the lineage of the muon by repeatedly getting the mother particle until there are no more ancestors (`imother < 0`). This line fetches the mother particle using its index (`imother`). It calculates the absolute value of the PDG code for the mother particle and checks if the particle is primary using the `AliAnalysisMuonUtility::IsPrimary()` method. If the mother particle is primary and its PDG code corresponds to a pion (PDG code 211) or kaon (321), it returns `kTRUE`. It then updates the mother particle index for

the next iteration. If no primary pion ancestor is found, the function returns `kFALSE`.

```
1 // Check if the particle is within the muon spectrometer acceptance
2 if(!IsWithinMuonSpectrometerAcceptance(fTrack))
3     continue;
4
5 // Fill the pT histogram (all particles) if in acceptance
6 fHistPtWAcc->Fill(fTrack->Pt());
7
8 // If it is a muon track, fill the muon pT histogram
9 if(fTrack->IsMuonTrack())
10     fHistMuPtWAcc->Fill(fTrack->Pt());
11
12 // Check if the muon track matches the trigger
13 if(!IsMuonTrackMatchingTrigger(fTrack))
14     continue;
15
16 // Calculate the pDCA of the particle/track
17 CalculatePDCA(fTrack);
18
19 // Apply pDCA cut
20 if(!IsPDCASelected(fTrack))
21     continue;
```

Listing A.7 Analysis Loop Initialization

A.2 Run Lists

APPENDIX B

Muon Yield

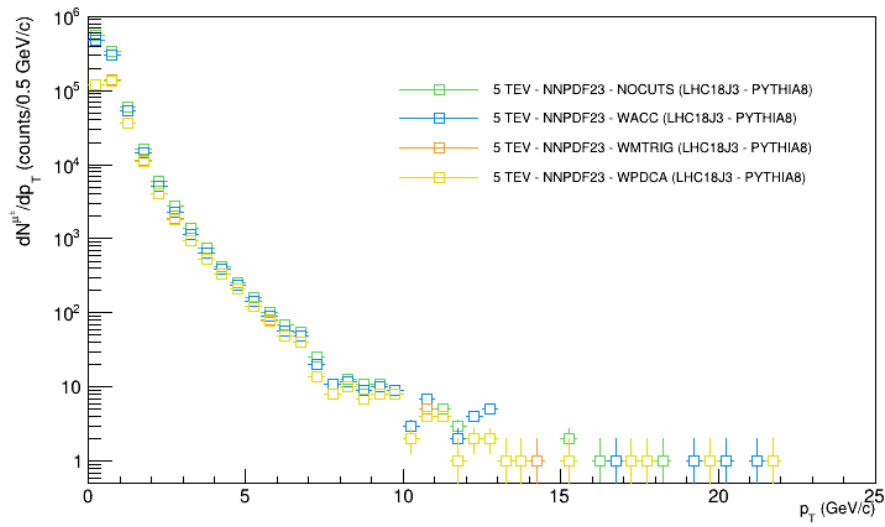


Fig. B.1 This plot illustrates the differential yield of all muons (inclusive) as a function of transverse momentum, generated using the PYTHIA 8 event generator with the NNPDF 2.3 parton distribution function, within the AliRoot framework for the ALICE experiment at a center-of-mass energy of 5 TeV.

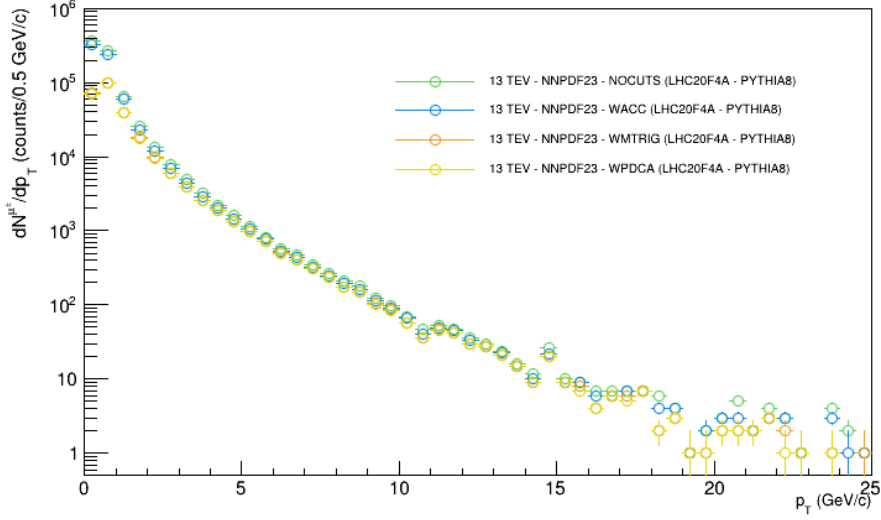


Fig. B.2 This plot presents the differential yield of all muons (inclusive) as a function of transverse momentum, generated by the PYTHIA 8 event generator with the NNPDF 2.3 parton distribution function. It is based on the AliRoot Monte Carlo production from the ALICE experiment at a center-of-mass energy of 13 TeV. The data spans the full spectrum of transverse momentum to illustrate the distribution of muon production rates.

The differential yield of all muons (inclusive), as a function of transverse momentum (p_T), is shown in the plots above (i.e., figures ?? and ??). The data points for muons at $\sqrt{s} = 13$ TeV are represented by circles, and those at $\sqrt{s} = 5.02$ TeV by squares. The horizontal lines at each data point represent the p_T bin width, while the vertical lines represent the statistical errors, illustrating the uncertainties associated with each measurement.

In both figures, ?? and ??, a clear distinction is observed in the inclusive muon yields at each center-of-mass energy before and after acceptance cuts are applied. This separation indicates the influence of the selection criteria on the observed yields. We note that the yield trends of muons decay similarly with increasing p_T at both energy levels. Specifically, the yield from the NNPDF 3.0 distribution is higher across the entire transverse momentum range, asserting a consistent divergence from other Parton Distribution Functions (PDFs) after the p_T surpasses 3 GeV/c. This trend is maintained throughout the higher p_T spectrum. Conversely, the CTEQL PDF consistently shows the lowest yield of muons before and after the application of acceptance cuts. Prior to the acceptance cuts (i.e, no cuts) at $\sqrt{s} = 5.02$ TeV, all PDF yield distributions were fairly consistent with each other, with very little difference. However, beyond $p_T > 3$ GeV/c, the NNPDF 3.0 yield begins to diverge from the rest, signifying a distinct behavior in response to the transverse momentum and acceptance cuts.

B.0.0.1 Muons from Primary Pion/Kaon Decays

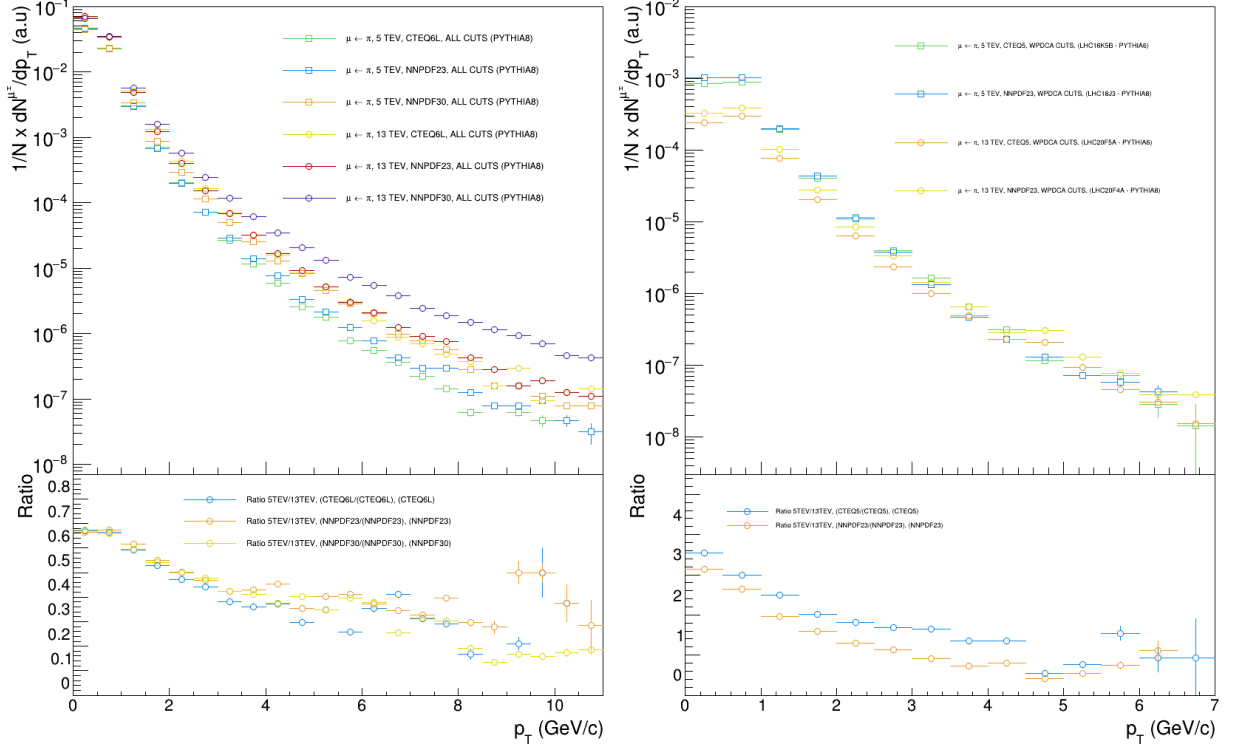


Fig. B.3 Normalised transverse momentum distributions of muons from primary pion decays at two center-of-mass energy levels, $\sqrt{s} = 5.02$ TeV and $\sqrt{s} = 13$ TeV. The left plot shows data from standalone PYTHIA 8 MC productions using CTEQ6L, NNPDF2.3, and NNPDF3.0 PDFs, while the right plot compares results from ALICE MC productions using AliRoot with CTEQ5 and NNPDF2.3 PDFs.

Moving to the analysis of muons from primary pion decays using standalone PYTHIA 8, we note the energy ratios follow a decreasing trend. This trend spans from a maximum of approximately 0.6 at $p_T = 0.5$ GeV/c, to an estimated low of 0.2 at around $p_T = 9$ GeV/c. Initially, the energy ratios of all the parton distribution functions (PDFs) appear to cluster together within the transverse momentum range of 0-1 GeV/c. However, the CTEQ6L energy ratio drops below the others at approximately $p_T = 1.5$ GeV/c.

As we extend our focus beyond $p_T > 1$ GeV/c, a divergence in the energy ratios emerges, with the NNPDF 2.3 ratio persistently higher, NNPDF 3.0 intermediate, and CTEQ6L maintaining the lowest ratio in the 1.5-2.5 GeV/c p_T range. Following this, CTEQ6L's energy ratio consistently remains the lowest throughout the rest of the p_T spectrum. We also encounter an inconsistency regarding which energy ratio (between NNPDF 2.3 and NNPDF 3.0) remains the highest for muons from primary pion decays. The most pronounced decrease in energy ratios is observed between p_T of 1 to 2.5 GeV/c, with a

noted moderation in the rate of decrease from the p_T range of 2 to 6 GeV/c, which might be influenced by the limited statistics available at p_T values higher than 4 GeV/c.

The AliRoot framework displays a downward progression in energy ratios for both examined PDFs. The peak values start around 3.6 for CTEQ5 and approximately 3.4 for NNPDF 2.3, both at $p_T = 0.5$ GeV/c. Conversely, minimum values are observed around 0.7 for CTEQ5 and 0.6 for NNPDF 2.3, both at $p_T = 5$ GeV/c. Throughout the entire p_T spectrum, the energy ratio for CTEQ5 remains above that of NNPDF 2.3. The most steeply sloped declines in energy ratios for both PDFs are between p_T of 0 and 2 GeV/c. Beyond this, the rate of decrease slows, reaching a plateau indicative of statistical limitations. CTEQ6L displays the most significant relative drop in energy ratios, suggesting a sensitive dependence on p_T for muons from primary pion decays.

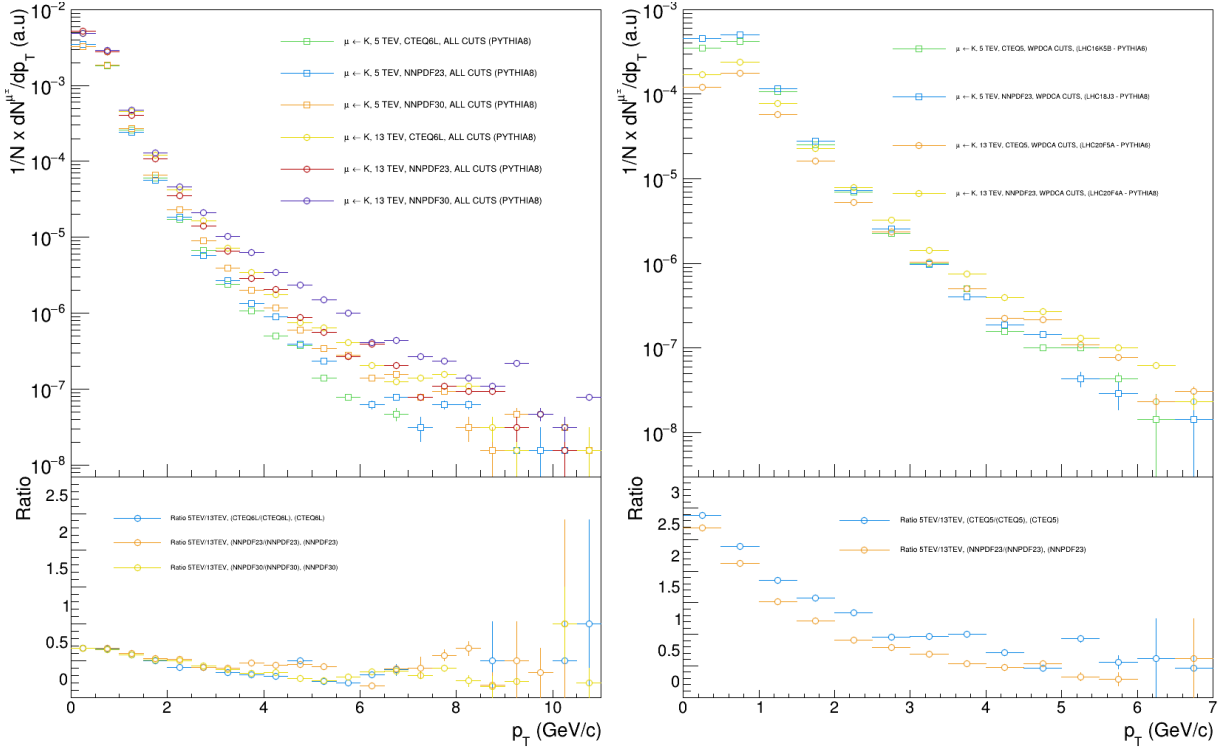


Fig. B.4 Normalised transverse momentum distributions of muons from primary kaon decays at two center-of-mass energy levels, $\sqrt{s} = 5.02$ TeV and $\sqrt{s} = 13$ TeV. The left plot presents results from standalone PYTHIA 8 MC productions using CTEQ6L, NNPDF2.3, and NNPDF3.0 PDFs, while the right plot features data from ALICE MC productions using AliRoot with CTEQ5 and NNPDF2.3 PDFs.

For muons originating from primary kaon decays analysed within the standalone PYTHIA 8 MC simulations, we note that the energy ratios also exhibit a declining trend. Starting from an approximate high of 0.7 at $p_T = 0.5$ GeV/c, the ratios descend to a low of about 0.2 at $p_T \approx 6.5$ GeV/c. In the p_T range of 0-2 GeV/c, the energy ratios of all PDFs show

similarity, yet the CTEQ6L ratio descends below the others at approximately $p_T = 2.5$ GeV/c.

Beyond $p_T > 2$ GeV/c, there is an inconsistent pattern of divergence among the energy ratios. NNPDF 2.3 mostly maintains the highest ratio up to $p_T = 5.5$ GeV/c, with NNPDF 3.0 generally in the middle, and CTEQ6L predominantly the lowest, though peaking at the $p_T = 5$ GeV/c bin. Continuing from this point, the energy ratio for CTEQ6L remains the lowest across the p_T spectrum. This inconsistency in which energy ratio prevails as the highest between NNPDF 2.3 and NNPDF 3.0 is particularly notable for muons from primary kaon decays. The sharpest drop in energy ratios occurs from p_T of 1 to 2 GeV/c, with the aforementioned irregularity in the trend of energy ratios becoming evident up to $p_T = 6$ GeV/c. Additionally, it is observed that the decrease in energy ratios for muons from primary kaon decays is slower in comparison to all muons and pion decays across all PDFs.

Within the AliRoot framework, a downward trajectory is again seen in the energy ratios for both PDFs. Maximum values are noted around 2.9 for CTEQ5 and approximately 2.7 for NNPDF 2.3, both at $p_T = 0.5$ GeV/c. The minimum values observed are roughly 0.8 for CTEQ5 and about 0.5 for NNPDF 2.3, both at $p_T = 4.5$ GeV/c. Throughout the entire transverse momentum spectrum, CTEQ5's energy ratio persists above that of NNPDF 2.3. The steepest decrease for both PDFs is seen between p_T of 0 and 2.5 GeV/c. Beyond this range, the decline in energy ratios moderates, yet for NNPDF 2.3 this trend continues uniformly, while for CTEQ5, irregularities become apparent once the data reach a region of limited statistics. In summary, NNPDF 2.3 exhibits the most stable and highest energy ratio across various p_T bins for muons from primary kaon decays. CTEQ6L shows a consistent pattern of having the lowest energy ratios, indicating a sensitivity in its response to changes in transverse momentum for muons from primary kaon decays.

B.1 Comparison of

B.1.0.1 Muons from Primary Pion/Kaon Decays

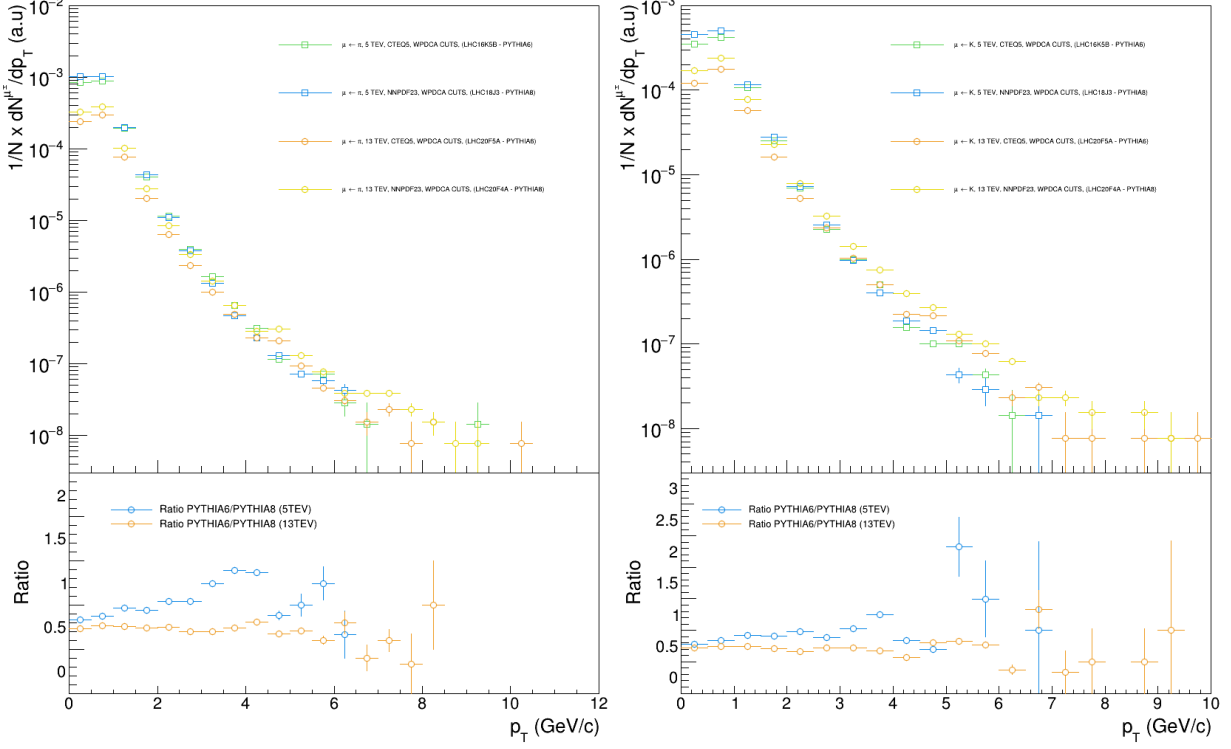


Fig. B.5 Normalised yield for muons from primary pions (left) and kaons (right) at $\sqrt{s} = 5.02$ TeV and $\sqrt{s} = 13$ TeV. The plots compare the muon production from pions and kaons using AliRoot (PYTHIA 6 vs PYTHIA 8) MC simulations with CTEQ5 and NNPDF2.3 PDFs.

When examining the normalised yields of muons resulting from primary pion decays, a notable decline in statistical reliability is evident beyond a transverse momentum of $p_T > 6$ GeV/c. At a center-of-mass energy of 5.02 TeV, the normalised yield is approximately 0.8 at $p_T = 0.5$ GeV/c and exhibits a gradual increase with escalating p_T , peaking around 1.4 at $p_T = 4$ GeV/c. This peak is followed by a minor drop at $p_T = 4.5$ GeV/c and then a larger drop from approximately 1.4 to 0.8 at $p_T = 5$ GeV/c. Beyond this point, the statistics become too limited to deduce a clear trend. At a center-of-mass energy of 13 TeV, the initial yield is observed to be around 0.7 at $p_T = 0.5$ GeV/c, with a peak noted at $p_T = 4.5$ GeV/c where the ratio reaches 0.8. The profile of the yield curve remains relatively stable, oscillating within a narrow bracket of 0.7 to 0.8. Past $p_T = 4.5$ GeV/c, the sharpest decrease in the ratio is recorded, although it is modest when contrasted with the variability observed at $\sqrt{s} = 5.02$.

The trend lines for the normalised yield ratios of muons from primary pion decays at different center-of-mass energies diverge in behavior. Specifically, at $\sqrt{s} = 5.02$ TeV, PYTHIA 6 is shown to produce a more substantial yield of muons from pion decays than PYTHIA 8 in the p_T range of 2 to 4.5 GeV/c. However, as the center-of-mass energy is increased, the trend shifts. At higher energies, the ratio for PYTHIA 6 relative to PYTHIA 8 does not surpass 0.8. The data suggests that PYTHIA 6 has a propensity to generate a higher yield of low- p_T muons from primary pions at lower center-of-mass energies. Conversely, at higher center-of-mass energies, PYTHIA 6's relative production diminishes and becomes more consistent, while PYTHIA 8 appears to yield more muons from primary pion decays. This observation may indicate an energy-dependent behavior in the muon production efficiency of the two PYTHIA versions, with PYTHIA 6 favoring lower energies and PYTHIA 8 showing advantages at higher energies.

In the context of the normalised yield spectrum of muons derived from primary kaon decays, we encounter limitations in the statistical dataset beyond a transverse momentum of $p_T > 5$ GeV/c. The pattern exhibited by kaons is similar to that observed for pions. At $\sqrt{s} = 5.02$ TeV, the initial normalised yield ratio of muons from kaon decays starts at approximately 0.8 at $p_T = 0.5$ GeV/c. This ratio then incrementally rises with an increase in p_T , reaching a peak around 1.3 at $p_T = 4$ GeV/c. Subsequently, a pronounced decline to roughly 0.8 at $p_T = 4.5$ GeV/c is observed, followed by a more gradual decrease to about 0.7 at $p_T = 5$ GeV/c. In the p_T range of 3 to 5 GeV/c, PYTHIA 6 is noted to generate a greater normalised yield of muons from kaon decays compared to PYTHIA 8, which is a similar increase in the ratio curve as noted with pions.

At $\sqrt{s} = 13$ TeV, the ratio pattern is again similar to that seen with pions, presenting a relatively constant and flat profile with minimal fluctuation. Starting at approximately 0.7 at $p_T = 0.5$ GeV/c, the ratio remains above 0.6 and does not exceed 0.8 within the 0 to 6 GeV/c range. Within the 0 to 4 GeV/c transverse momentum range, the ratio is tightly constrained between approximately 0.7 and 0.8. For PYTHIA 6, a higher normalised yield of muons from kaon decays is consistently produced within a specific p_T range. However, with an increase in the center-of-mass energy, a contrasting outcome is observed: the yield ratio of PYTHIA 6 to PYTHIA 8 does not surpass 0.8. This discrepancy suggests that PYTHIA 6 may preferentially enhance the production of low- p_T muons from kaon decays at lower energies, whereas at higher energies, the relative production stabilises and PYTHIA 8 emerges as a more prolific source of muons from kaon decays within the same p_T spectrum.

B.2 Effects of Accurate Detector Simulation

B.2.0.1 Muons from Primary Pion/Kaon Decays

See note above.

B.2.0.2 Muons from Heavy-Flavour Decays

See note above.

B.2.1 Comparison of PDFs

In this section, we analyse the impact of different PDFs on the normalised yields of muons as a function of transverse momentum. The study ensures that the center-of-mass energy and PYTHIA version remain constant while the PDFs vary, thereby isolating the effect of PDF selection on muon production. For each set of conditions where the energy and PYTHIA version match but the PDFs differ, a ratio of the corresponding histograms is computed. This ratio is designed to reveal the relative influence of the PDFs on the normalised yields.

B.2.1.1 All Muon Sources

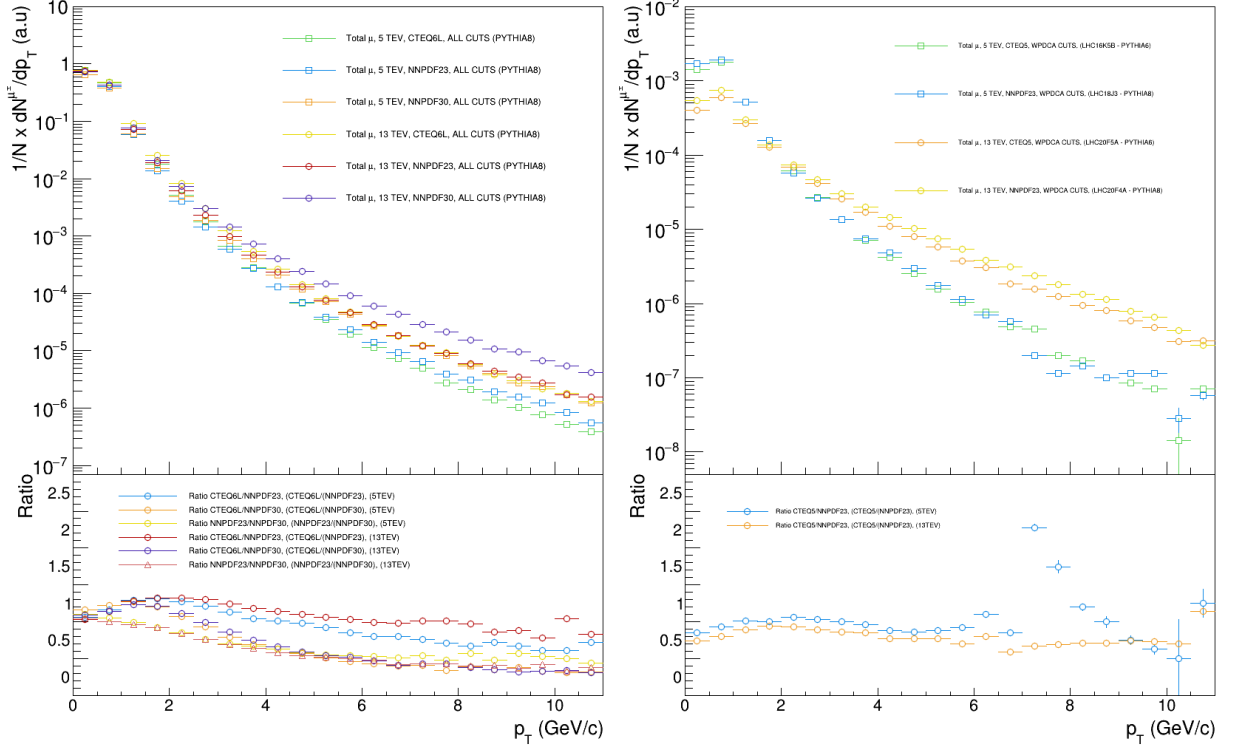


Fig. B.6 Normalised transverse momentum distributions of muons from all sources, comparing the impact of different PDFs at $\sqrt{s} = 5.02$ TeV and $\sqrt{s} = 13$ TeV. The left plot illustrates data from standalone PYTHIA 8 MC productions with CTEQ6L, NNPDF2.3, and NNPDF3.0, while the right plot depicts data from ALICE MC productions using AliRoot with CTEQ5 and NNPDF2.3.

B.2.1.2 Muons from Primary Pion/Kaon Decays

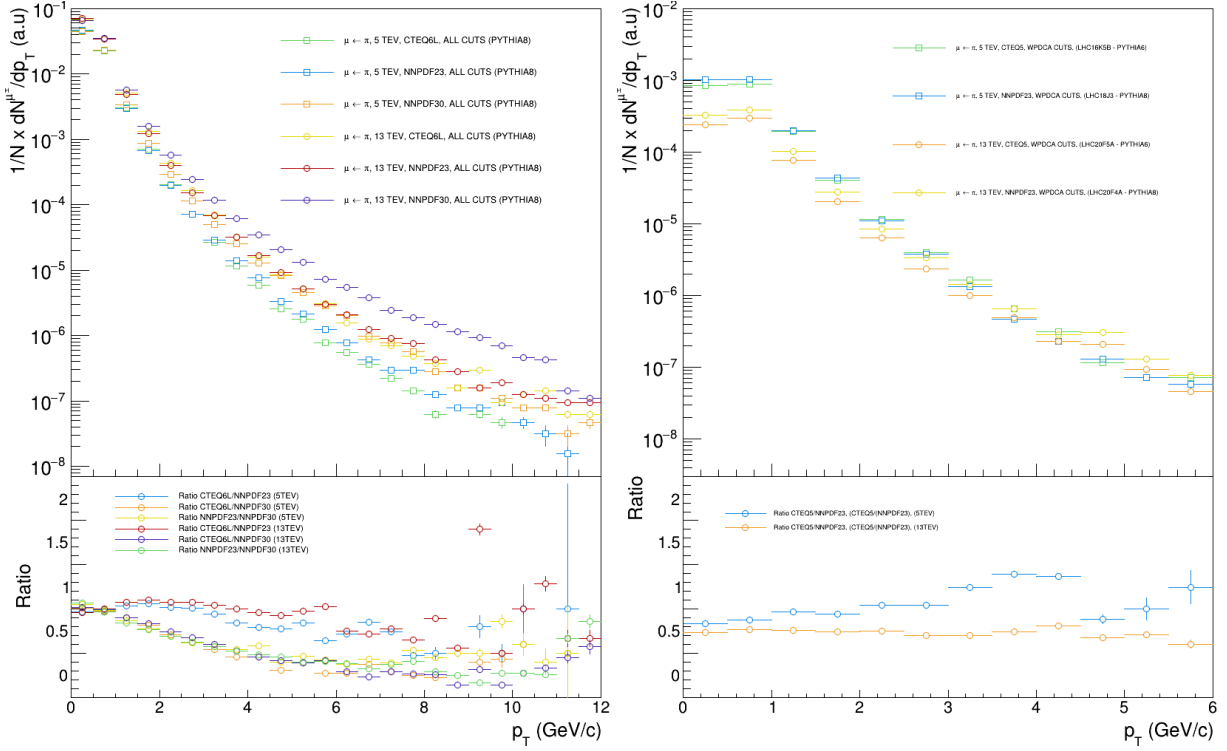


Fig. B.7 Normalised transverse momentum distributions of muons from primary pion decays, comparing the impact of different PDFs at $\sqrt{s} = 5.02$ TeV and $\sqrt{s} = 13$ TeV. The left plot presents data from standalone PYTHIA 8 MC productions with CTEQ6L, NNPDF2.3, and NNPDF3.0, while the right plot features data from ALICE MC productions using AliRoot with CTEQ5 and NNPDF2.3

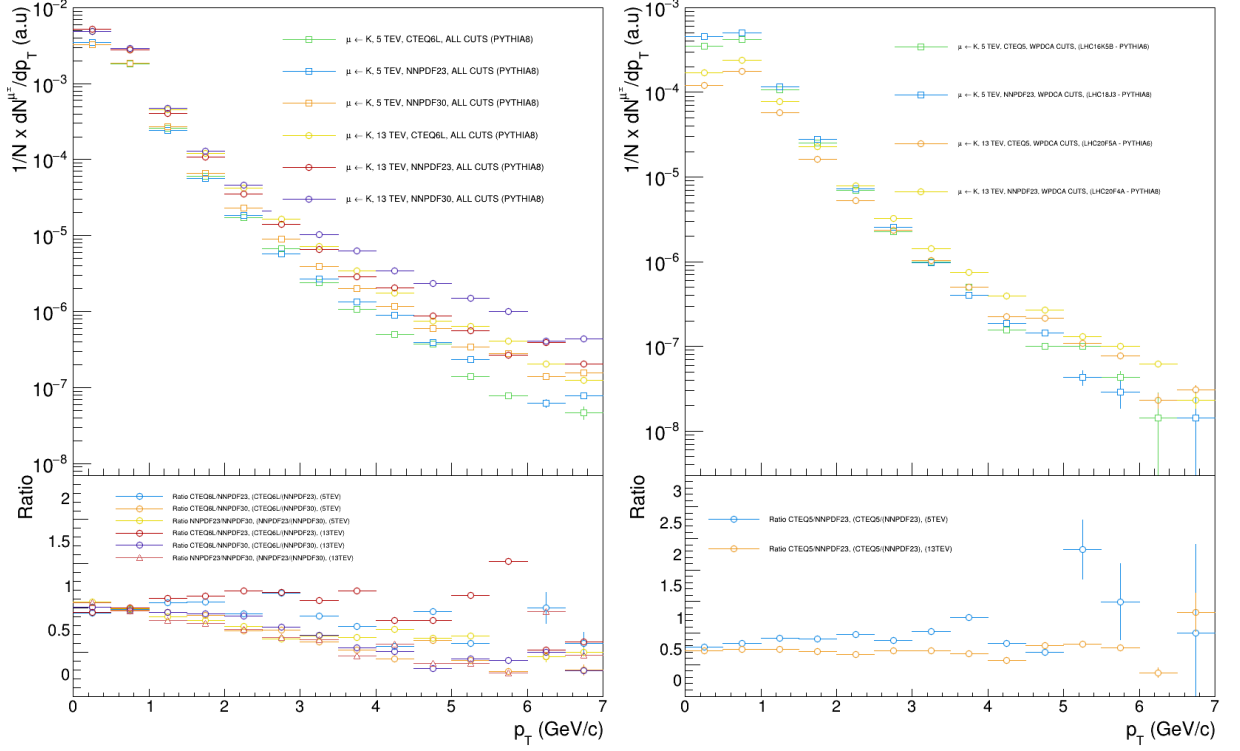


Fig. B.8 Normalised transverse momentum distributions of muons from primary kaon decays, comparing the impact of different PDFs at $\sqrt{s} = 5.02$ TeV and $\sqrt{s} = 13$ TeV. The left plot shows results from standalone PYTHIA 8 MC productions with CTEQ6L, NNPDF2.3, and NNPDF3.0, and the right plot includes data from ALICE MC productions using AliRoot with CTEQ5 and NNPDF2.3.

B.3 Primary Charged Pion and Kaon Background

In this part of the study, we delve into the role that muons from primary charged pions and kaons play as background noise in the analysis of heavy-flavour decay signals. Our focus is specifically on the 0 to 12 GeV/c transverse momentum range, which is a critical window for observing these background contributions. The approach adopted here is to utilise the normalised muon yield data from pion and kaon decays as it is, comparing it against the overall muon yield. This direct comparison allows for an assessment of the background's impact relative to the entire muon population in our dataset.

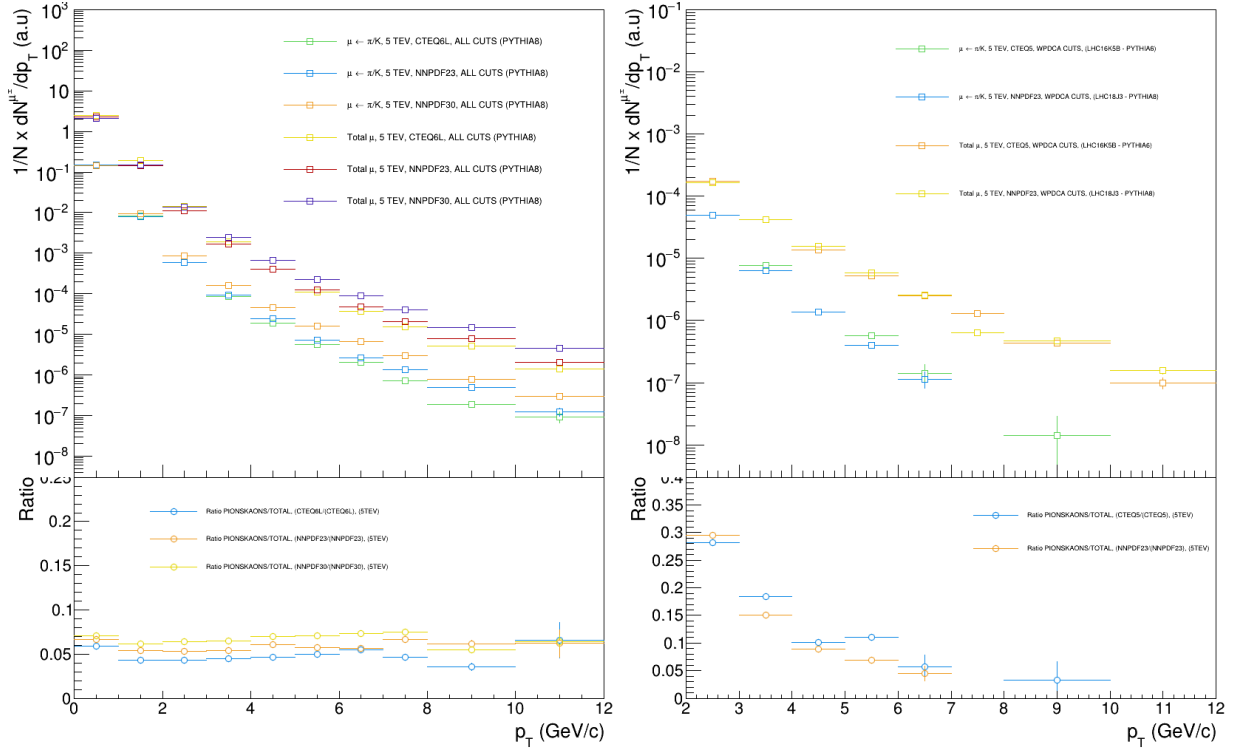


Fig. B.9 Normalised yield distributions of muons from primary pion and kaon decays compared to the total muon yield at $\sqrt{s} = 5.02$ TeV, with the bottom ratio plot indicating the background fraction. The left plot utilises standalone PYTHIA 8 across multiple PDFs, and the right plot features AliRoot simulations with PYTHIA 8, detailing the proportion of background contributions from pion and kaon decays.

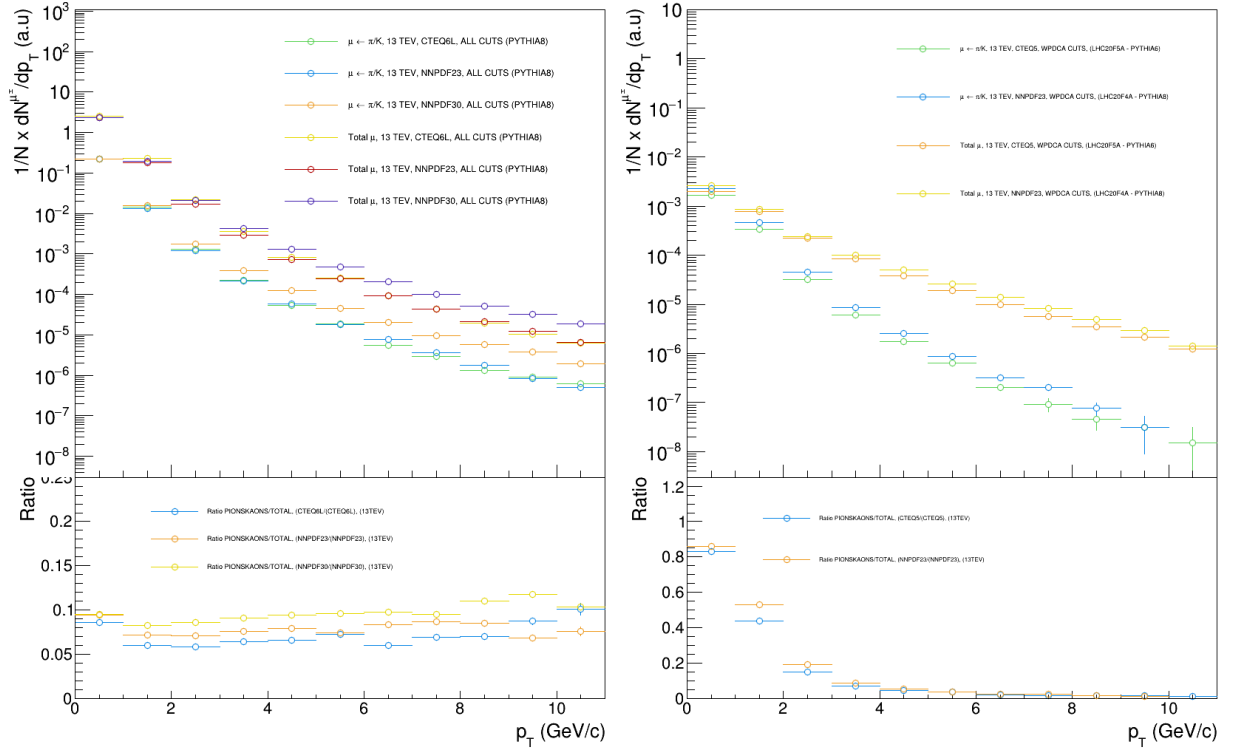


Fig. B.10 Normalised yield distributions of muons from primary pion and kaon decays relative to the total muon yield at $\sqrt{s} = 13$ TeV, with the lower ratio plot reflecting the background fraction. Standalone PYTHIA 8 simulations with various PDFs are displayed on the left, while the right plot visualises AliRoot simulations with PYTHIA 8, both quantifying the background fraction from pion and kaon decays in the overall muon data.